Journal of Electronic Materials (2022) 51:3042–3058
https://doi.org/10.1007/s11664-022-09476-z

ORIGINAL RESEARCH ARTICLE

Comparative Study of the Effects of La-Substituted Ca in (Bi, Pb):2212 and (Bi, Pb):2223 Superconductors

A. Sedky[1] · Amna Salah[1]

Received: 14 October 2021 / Accepted: 24 January 2022 / Published online: 16 March 2022

Abstract

We report here a comparative study of the effects of La-substituted Ca on (Bi, Pb):2212 and (Bi, Pb):2223 superconductors with various La content ($0.00 \leq x \leq 0.30$). Regardless of the effects of La, it is evident that the superconducting volume fraction, excess of oxygen, critical concentration for quenching superconductivity, Vickers hardness, anisotropy, interlayer coupling, critical magnetic fields, and critical current were higher for the 2212 series than the 2223 series. In contrast, orthorhombic distortion, c-parameter, crystallite diameter, doping distance, distance between two Cu atoms, hole carrier/Cu ion ratio, melting temperature T_m, critical temperature T_c, onset of diamagnetic T_{cM}, surface energy, elastic component, resistance pressure, and c-axis coherence length were higher for the 2223 series than the 2212 series. An inverse linear relationship between T_m and T_c was estimated for both series, and for room-temperature (RT) bismuth–strontium–calcium–copper–oxide (BSCCO) superconductors, the required T_m values should be 1048.03°C for the 2223 series and 784.48°C for the 2212 series. Surprisingly, the difference in temperature between zero resistivity and diamagnetic onset $|T_{cM} - T_{cR}|$ for La = 0.30 samples is 30 K. In the critical field region (CFR), the exponents of order parameters (OPD) are two-dimensional (2D), but their values were higher for the 2212 series than the 2223 series. Further, they became three-dimensional (3D) as La increased to 0.30 due to the reduced effective length in highly substituted samples. Our results were discussed with the help of the differences in the physical parameters between the considered series. These findings revealed that the 2212 series is more suitable for applications that need higher hardness and critical fields and currents. In contrast, the 2223 series is more suitable for research for higher T_c and altering plastic deformation. To our knowledge, the present systematic investigation has not been reported elsewhere, which highlights the present work.

Keywords BSCCO phases · excess oxygen · hole carrier/Cu · excess conductivity · Vickers hardness · melting point · critical temperature

Introduction

The (Bi, Pb):2212 orthorhombic unit cell consists of two units of (Bi, Pb)$_2$Sr$_2$CaCu$_2$O$_8$ and 15 layers. The oxygen atoms of ($8O^{2-}$) need 16 electrons, which are supplied by the $2Bi^{3+}+2Sr^{2+}+1Ca^{2+}+2Cu^{2+}$. To be a superconductor, the cell is over-doped with excess oxygen δ of 0.10–0.23.[1] The extra atom requires two more electrons through transforming two Cu^{2+} ions into two Cu^{3+} ions, and therefore, the electronic arrangement in the unit cell has two CuO_2 planes and becomes $2Bi^{3+}+2Sr^{2+}+1Ca^{2+}+2Cu^{3+}+9O^{2-}$. In contrast, the unit cell of the Bi (Pb):2223 compound consists of a $Bi_{1.7}$ Pb $_{0.30}Sr_2Ca_2Cu_3O_{10+\delta}$ unit and about 19 layers and planes. The chemical formula of ten oxygen atoms (10 O^{2-}) requires at least 20 electrons, which are supplied by $1.7Bi3^{+}+0.30Pb^{2+}+2Sr^{2+}+2Ca^{2+}+3Cu^{2+}$. To be a superconductor, it is over doped with excess oxygen by transforming three Cu^{2+} ions into three Cu^{3+} ions, and therefore, the electronic arrangement having three CuO_2 planes becomes $1.7Bi^{3+}+0.30Pb^{2+}+2Sr^{2+}+2Ca^{2+}+3Cu^{3+}+11O^{2-}$.[2]

The Bi (Pb):2212 and Bi (Pb):2223 superconductors, with critical temperatures (T_C) of 87 and 110 K, respectively, have been widely used in the fabrication of wires and tapes due to their high critical fields and currents.[3,4] Usually, the low Bi:2201 and Bi:2212 phases tend to coexist as minority phases with (Bi, Pb):2212 and (Bi, Pb):2223 majority phases, but the calcination process

✉ A. Sedky
sedky196000@hotmail.com; sedky1@aun.edu.eg

[1] Physics Department, Faculty of Science, Assiut University, Assiut 71516, Egypt

depresses as much as possible the number of minority phases.[5–7]

Numerous studies on the effects of RE^{3+} substitutions at the Ca^{2+} site in the BSCCO system (RE^{3+} rare earth element in the lanthanide series)[8–13] have been reported. It has been proved that such a substitution decreases the density of superconducting carriers in BSCCO systems, and consequently, the critical concentration x_c required for quenching superconductivity is decreased.[14–16] Further, the x_c decreases as the ionic size of RE^{3+} increases towards the La series. Meanwhile, other reports show an increase in the x_c by Y substitution in place of Ca.[17–19] But most of the research has been focused on the Y, Gd, Sm, and Nd elements,[20–24] and a few of them are based on the La element due to the poor superconductivity of La: 123.

However, the excess of positive charge for trivalent RE^{3+}cation, as compared to divalent Ca^{2+}cation, causes repletion between CuO_2 planes, thereby the separation between these planes may be increased. Furthermore, the increase in RE content induces excess oxygen to be incorporated between the Bi_2O_3 double layers.[25] In this respect, the oxygen stoichiometry of BSCCO systems is relatively invariant with respect to RE^{3+} when prepared in an identical environment.[26–28]

Recently, Sedky et al. presented individual studies on the structural, thermal, mechanical, electrical, magnetic, and excess conductivity properties of the $Bi_{1.7}Pb_{0.30}Sr_2Ca_{1-x}La_xCu_2O_y$ (2212) and $Bi_{1.7}Pb_{0.30}Sr_2Ca_{1-x}La_xCu_2O_y$ (2223) series.[29–32] It has been proved that La significantly improves the superconducting parameters related to both series and also extends the superconductivity above 0.30. This study presents a comparative analysis of the effects of La-substituted Ca in (Bi, Pb):2212 and (Bi, Pb):2223 superconductors. Regardless of the effects of La, it is concluded that superconducting volume friction, excess oxygen, x_c, Vickers hardness, critical fields, and currents are higher for the 2212 series than the 2223 series. In contrast, the melting temperature T_m, critical temperature T_c, onset of diamagnetic T_{cM}, surface energy, elastic component, and resistance pressure are higher for the 2223 series than the 2212 series. In addition, the order parameter exponents in the critical field region (CFR) are two-dimensional (2D) for both series, but their values are higher for the 2212 series than the 2223 series. Further, they become three-dimensional (3D) as La is increased to 0.30 due to the expected reduced effective length in highly substituted samples. Our results are discussed in terms of differences in the most calculated and measured superconducting parameters between the two series. To our knowledge, the present investigation has not been reported elsewhere, which highlights the present work.

Experimental Details

The Bi_2O_3, PbO, SrO, La_2O_3, CaCO3, and CuO oxides and carbonates of 4*N* purity were thoroughly mixed in the required proportions and calcined at 825°C in air for 24 h. This exercise was repeated three times, with intermediate grinding at each stage. The resulting powder was reground, mixed, and pressed into pellets at a force of up to 10 tons. The pellets of (Bi, Pb):2212 were sintered in air at 840°C for 36 h and left in the furnace for slow cooling to room temperature at a rate of 5°/min. (Bi, Pb):2223 pellets were also sintered in air at 850°C, but for 150 h and then left in the furnace for slow cooling at the same rate of 5°/min. The phase purity of the samples was examined using an X-ray diffraction pattern (XRD) using a Philips PW-1700 with Cu-Kα radiation of wavelength $\lambda = 1.5418$ Å at 40 KV and 30 mA settings and a diffraction angle range of 20°–70° with a step of 0.06°. Differential thermal analysis (DTA) and thermogravimetric analysis (TGA) of the samples in powder form were performed in the temperature range of 30–1000°C with a heating rate of 10°C/min. The electrical resistivity of the samples was obtained using the standard four-probe technique in a closed-cycle cryogenic refrigerator within the range of 18–300 K (Displex) employing helium gas. Direct-current (DC) magnetization was carried out by means of a SQUID magnetometer (Quantum Design) in both field cooling (FC) and zero-field cooling (ZFC) at a field of 20 Oe in the temperature range of 10–150 K. More precisely, the samples were first cooled to 20 K in the absence of the applied field, then the field was switched on and the data was acquired for increasing temperature (ZFC) up to 150 K. After that, the samples were cooled again and FC magnetization was acquired in the presence of the field. Finally, the Vickers microhardness of the samples at room temperature was determined using the manual microhardness tester model IN-412A with an applied load of 0.49–10 N for 10 s.

Results and Discussion

XRD and DTA Analysis

The XRD patterns of the samples shown in Fig. 1a and b show that the 2212 H (hkl) and 2223 H (hkl) superconducting phases were responsible for the majority of the obtained peaks, which correspond to $T_c = 89$ K and 110 K, respectively. In contrast, the minority peaks of very low intensity indicated by L (hkl) belong to the minority superconducting phases of Bi (Pb):2201 and Bi (Pb):2212, with T_c of 23 and 89, respectively, which are normally formed

during the synthesis of Bi (Pb):2212 and Bi (Pb):2223, respectively. In addition, they are formed with very lower intensities in BSCCO systems and therefore cannot be considered as impurity phases, consistent with the results reported elsewhere.[14,19,22,29,30]

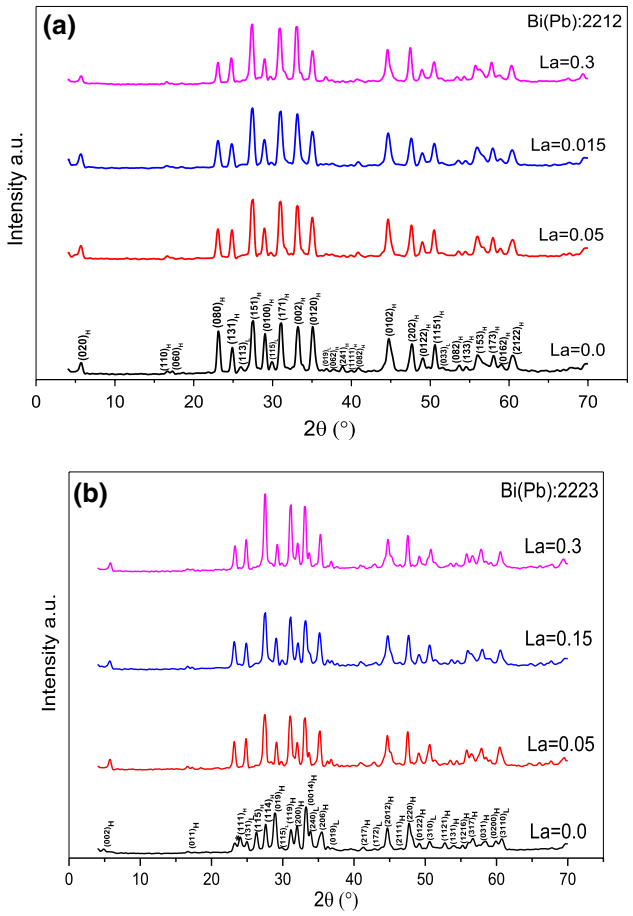

Fig. 1 XRD patterns for the samples (a) Bi (Pb):2212 (b) Bi (Pb);2223.

The superconducting volume fractions of the 2212 (V_{2212}) and 2223 (V_{2223}) series were determined by[7,33,34]

$$V_{2212} = \frac{\Sigma I_{2212}(\text{peaks})}{\Sigma I_{2212}(\text{peaks}) + \Sigma I_{2201}(\text{peaks}) + \Sigma I_{\text{other}}(\text{peaks})}$$

and

$$V_{2223} = \frac{\Sigma I_{2223}(\text{peaks})}{\Sigma I_{2223}(\text{peaks}) + \Sigma I_{2212}(\text{peaks}) + \Sigma I_{\text{other}}(\text{peaks})}, \quad (1)$$

respectively.

It is also clear from Fig. 2a that V_{2212} is higher than V_{2223}. This is because the 2201 minority phase formed in the 2212 series at 750°C, whereas the minority 2212 phase formed at 825–850°C in the 2223 series. As the temperature increased to the sintering point (850°C), the majority of the 2201 phases were transferred to 2212, and therefore V_{2212} was increased. In the case of the 2223 series, the amount of the 2212 minority phase was not completely transferred to the 2223 phase, which in turn decreased the 2223 majority phase. The porosity of the samples was calculated as $PS = [1 - (\rho_{exp}/\rho_{th})]$ and shown in Fig. 2b. It is seen that *PS* was decreased by La for both series, but it was higher for the 2223 series than the 2212 series. This behavior may be related to the ratio of dislocation density and oxygen vacancies between them, which may be higher for the 2223 series than for the 2212 series.

The c-parameter and orthorhombic distortion OD = [(b − a)/a] against La are shown in Fig. 3a and b for both series. It was found that the OD for pure 2212 was generally higher than that for 2223, while the opposite was true for the La-substituted samples. However, this was related to the amount of excess oxygen and the length of the Cu–O bond in the $Cu–O_2$ planes in both series, as reported elsewhere.[36–39] Consequently, the length of the in-plane Cu–O bond was decreased, which is helpful for more effectively reducing the a-parameter of pure 2212 as compared to pure 2223. Otherwise, the change in the b-parameter is related to the

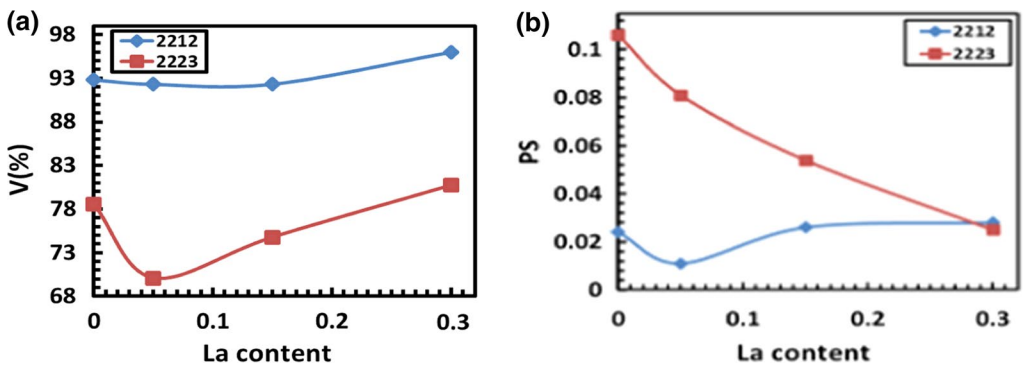

Fig. 2 (a) Superconducting volume fraction (V%) versus La content for the samples. (b) Porosity *PS* versus La content for the samples.

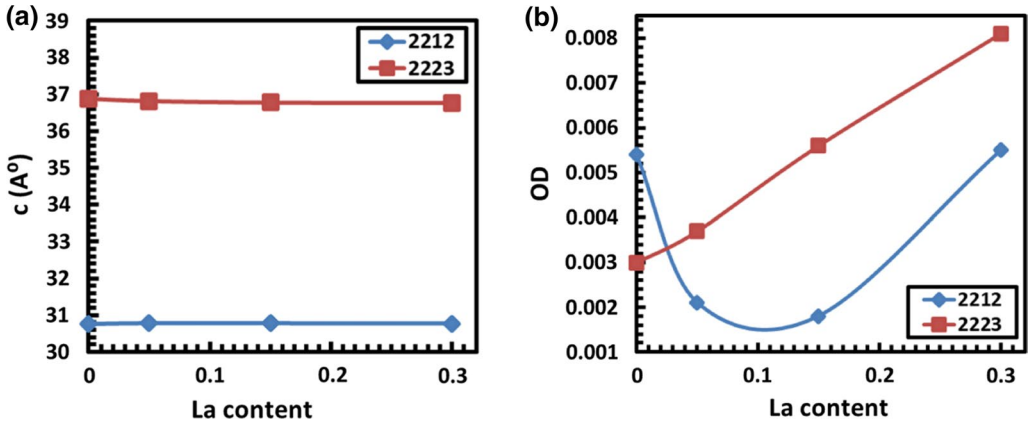

Fig. 3 (a) c-lattice parameter versus La content for the samples. (b) orthorhombic distortion (OD) versus La content for the samples.

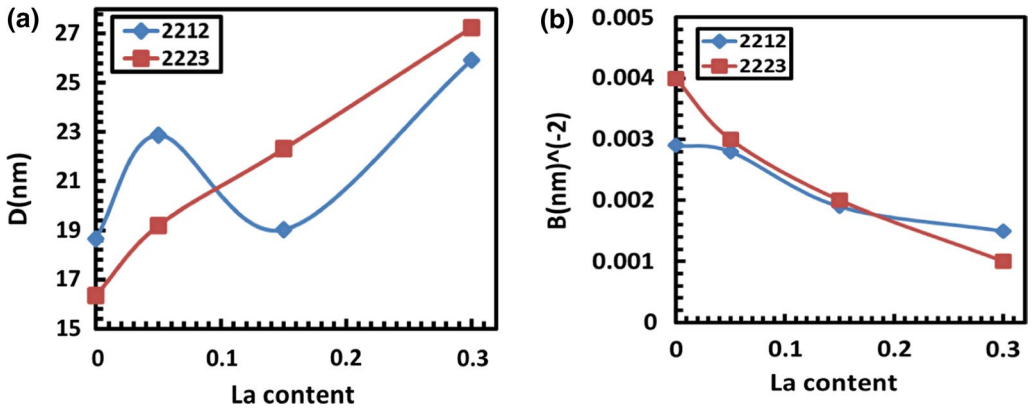

Fig. 4 (a) Crystallite size (D) versus La content for the samples. (b) Dislocation density (β) versus La content for the samples.

change in the hole carrier concentration per Cu ion, which is induced by La doping within these planes.[40–43] Thus, the rate of decrease or increase in the (a/b) ratio for La-substituted samples is responsible for the further increase of OD in the 2223 series than that of the 2212 series. On the other hand, the c-parameter of the 2223 series was higher than that of the 2212 series. This was due to increasing the number of CuO_2 planes in 2223 (three planes) as compared to 2212 (two planes).

The average crystallite diameter, D_{hkl}, evaluated by Scherer's equation, and also the dislocation density, $\beta = 1/D_{hkl}^2$, against La content are shown in Fig. 4a and b. D_{hkl} values are higher for pure 2212 and La = 0.05 samples than for similar samples of the 2223 aeries, while the opposite is true for La-substituted samples. This may be related to the behavior of V_{2212} and V_{2223} against La for both series. β values were decreased by La, and they were slightly higher for the 2223 series than the 2212 series. This behavior indicated that La samples have very few lattice defects and good crystalline quality.[44,45] Further, the increase in the 2223 series may be related to increasing both the c-parameter, OD, and D_{hkl}.

Figure 5a and b shows the DTA patterns of the samples. It is worth noting that when T was raised to around 800°C, the crystallization tendencies for 2201 in the 2212 series and 2212 in the 2223 series almost vanished. Figure 6a and b shows the heat loss and melting temperature T_m at the peak against the La content for both series. The heat loss of pure 2212 was higher than that of pure 2223 and decreased by La for both series, but it was higher for the 2223 series than the 2212 series. This result indicated that the amount of 2201 minority phase formed in the 2212 series was melted below 800°C and after that it decomposed into the 2212 majority phase.[46] In contrast, the 2212 minority phase formed in the 2223 series was melted above 800°C, and after that, it decomposed into the 2223 majority phase.[47] The T_m was increased by La for both series, but it was higher for the 2223 series than the 2212 series even for pure samples. This may be attributed to increasing the optimum temperature required for melting the mixture due to La, which facilitated the growth of majority phases.[47,48] Such an observed increase in T_m emphasizes the role of La addition in the internal structure of the examined samples.

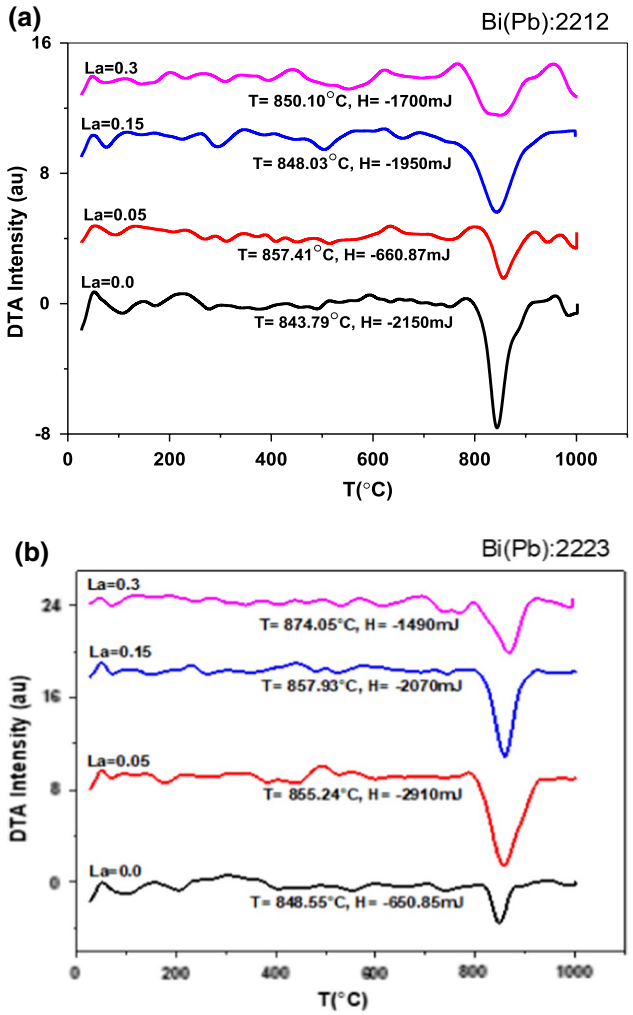

Fig. 5 DTA pattern versus temperature for the samples (a) Bi (Pb):2212 and (b) Bi (Pb):2223.

Oxygen Content Analysis

Figure 7a shows the oxygen content y against the La content for both series, and it is seen that for pure samples, there is an excess of oxygen above the stoichiometric values of 8 and 10 for both systems ($y = 8.1$ for 2212 and 10.07 for 2223). Furthermore, values of y were gradually increased by La for the two series, but it is higher for the 2223 series than the 2212 series, which indicates that La helps with more excess oxygen for the two series. For more clarity, the excess oxygen is 0.10, 0.17, 0.47, and 0.58 for 2212, which is higher than 0.07, 0.12, 0.37, and 0.53 determined for 2223, as well as the OD behavior obtained from XRD. However, according to the mechanism of excess oxygen in a pure BSCCO system, the electrons were transferred from Cu to the BiO layer, leading to the formation of holes on Cu and electrons on Bi according to $Bi^{3+}+Cu^{2+} \rightarrow Bi^{3-x}+Cu^{2+x}$. These changes in the valence state of Bi are due to excess oxygen and are reflected as the changes of hole carriers in the $Cu–O_2$ planes. Since the superconductivity of copper-oxide systems is localized in the $Cu–O_2$ planes where the majority of holes are supposed to reside, it is believed or expected that the majority of excess of oxygen will be in the $Cu–O_2$ planes.

The effective Cu^{eff} valance was obtained by

$$Cu^{eff} = \frac{2y - [9.7 + 2(1-x) + 3x]}{2}; \quad \text{for} \quad 2212; \quad \text{and}$$
$$Cu^{eff} = \frac{2y - [9.7 + 2(2-x) + 3x]}{2}; \quad \text{for} \quad 2223 \qquad (2)$$

Figure 7b shows the Cu^{eff} against La for the two series. It was found that the values of Cu^{eff} are higher for the 2223 series than the 2212 series. This can be explained in terms of increasing the number of holes which may be introduced by La as a result of such substitution. Thus it is illogical to replace Ca^{2+} by La^{3+}, and therefore, Cu^{eff}, should be decreased, but this is discussed in the next paragraph.

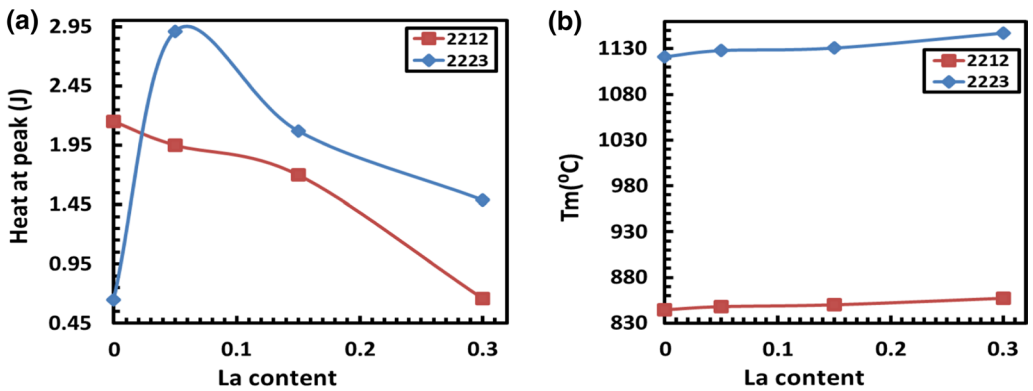

Fig. 6 (a) Heat at the peak versus La content for the samples. (b) Melting temperature (T_m) versus La content for the samples.

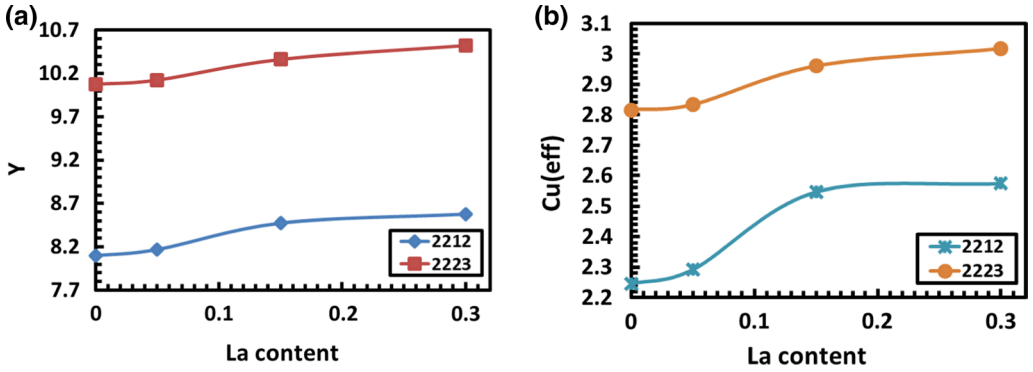

Fig. 7 (a) Oxygen content (Y) versus La content for the samples. (b) Effective Cu valance (Cu_{eff}) versus La content for the samples.

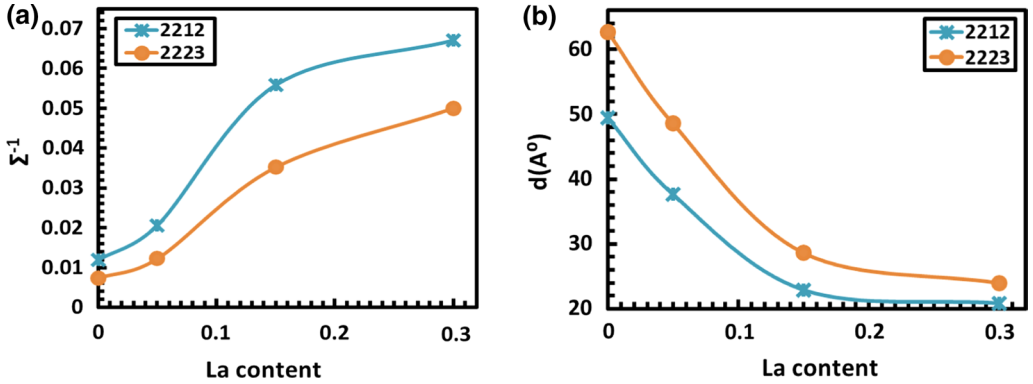

Fig. 8 (a) Excess doping density (Σ^{-1}) versus La content for the samples. (b) Doping distance (d) versus La content for the samples.

The excess oxygen in the form of excess doping density Σ^{-1} is converted into a doping distance d as follows[23,49]:

$$d = a\sqrt{\sum} \tag{3a}$$

where a is lattice parameter, and Σ given by

$$\Sigma = \frac{1}{(1-8y^{-1})}; \quad \text{for} \quad 2212; \quad \text{and}$$
$$\Sigma = \frac{1}{(1-10y^{-1})}; \quad \text{for} \quad 2223 \tag{3b}$$

It is evident from Fig. 8 that Σ^{-1} is higher for the 2212 series than the 2223 series, while d is higher for the 2223 series than the 2212 series; see Fig. 8a and b. This, of course, is clear evidence of changing the hole carrier concentrations between the series as a result of such substitution. Increasing d for the 2223 series rather than the 2212 series is related to the difference in the c-axis between them. The distance z between the two nearest Cu atoms was calculated by[23,50,51]

$$z = \sqrt{[(2a)^2 + a^2]} = a\sqrt{5} \tag{4}$$

Moreover, the crystal geometry factor (CGF) of the area of superconducting planes can be obtained from

$$\mathrm{CGF(Jm^2kg)} = [(2d)^2 n^{\frac{-3}{2}} 2\pi K_B T_c m_{eff}] = 6.31 \times 10^{-54} d^2 T_c n^{\frac{-3}{2}} \tag{5}$$

where n is the number of CuO_2 planes, and m_{eff} is the effective mass of the hole ($m_{eff} = 2m_e = 18.210^{-31}$ kg).

It is evident from Fig. 9a and b that z is higher for the 2223 series than the 2212 series. The CGF factor is higher for pure 2223 than for pure 2212, and the difference in CGF between them is gradually decreased by La until it becomes zero for La = 0.15 and 0.30 samples. This behavior can be considered good evidence for hole carrier behavior between the series, as presented in the next paragraph.

Resistivity Analysis

Figure 10a and b depicts the electrical resistivity versus temperature for the two series. Figure 11a depicts the critical T_c, onset temperature T_{on}, and transition width ΔT_c for the samples. It was found that T_c and T_{on} were higher

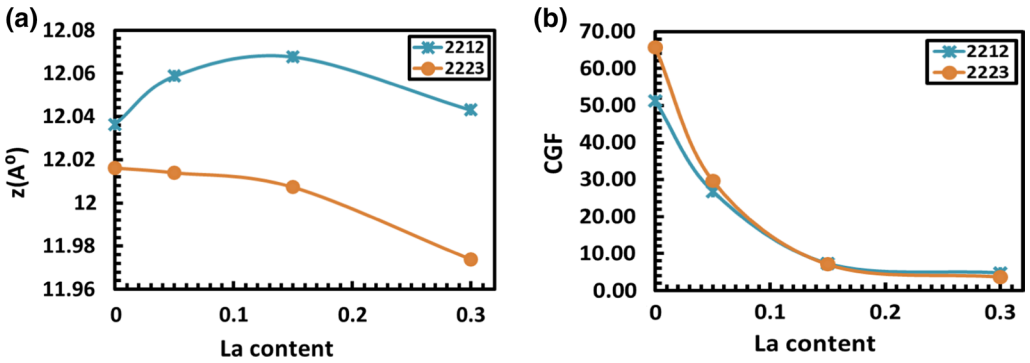

Fig. 9 (a) Distance between two nearest Cu atoms (z) versus La content for the samples. (b) Crystal geometry factor (CGF) versus La content for the samples.

for the 2223 series than the 2212 series. This was due to the difference in T_c for pure samples (94 K for 2212 and 119 K for 2223). The reduced T_c [$T_c(x)/T_c(0)$] against La is also shown in Fig. 11b. It was found that the critical concentration x_c of La for quenching superconductivity can be extended above 0.30 for both series, which is higher than that reported (0.25).[8–16,18–22,26,52,53] It was also clear that La slightly had a higher solubility in the 2212 series, and it was less detrimental to the superconductivity as compared to the 2223 series; that is $[T_c(x)/T_c(0)] \alpha (1/T_c)$ for BSCCO systems.

An inverse linear relation could be obtained between T_m obtained from DTA and T_c as shown in Fig. 12b. The linear relations are given by

$T_c(K) = -3.406\ T_m + 2963.3$ for 2212 and $T_c\ (K) = -2.5413\ T_m + 2963.3$ for 2223, which is consistent with reported values for high-T_c systems.[54,55] This finding suggests that to achieve a higher T_c, an eutectic compound with a lower melting point should be looked into. Based on the above data, a composition of $T_m = 784.48°C$ for 2212 and 1048.03°C for 2223 is required for RT superconductivity with $T_c = 300$ K.

The phase diagram of high-T_c systems is well described by[56]

$$\frac{T_c^m}{T_c^x} = 1 - 82.6(p - 0.16)^2 \quad (6)$$

where T_c^x and T_c^m are the critical and maximum T_c, respectively, and p is the hole carrier concentration per Cu ion. It is evident from Fig. 12a that p is higher for the 2223 series than the 2212 series due to the extra positive charges transferred to the CuO_2 planes, which disagrees with the role of substitution for decreasing P due to replacing Ca^{2+} by La^{3+}.[57,58] To clarify this point, we suppose that La decreases the hole carrier concentration due to replacing Ca^{2+} by La^{3+}, but in contrast, the excess oxygen introduces some excess holes in the Cu–O_2 planes, and consequently, the effective (net) number of holes is increased, but the rate of increase is higher in 2223 than in 2212. This can also be supported by the behavior of doping distance and density of excess doping presented above.

Magnetic Measurements

Figure 13a–d shows the magnetic moment as a function of temperature in the field cooling (FC) and zero field cooling (ZFC) for the samples. Although the diamagnetic signal is

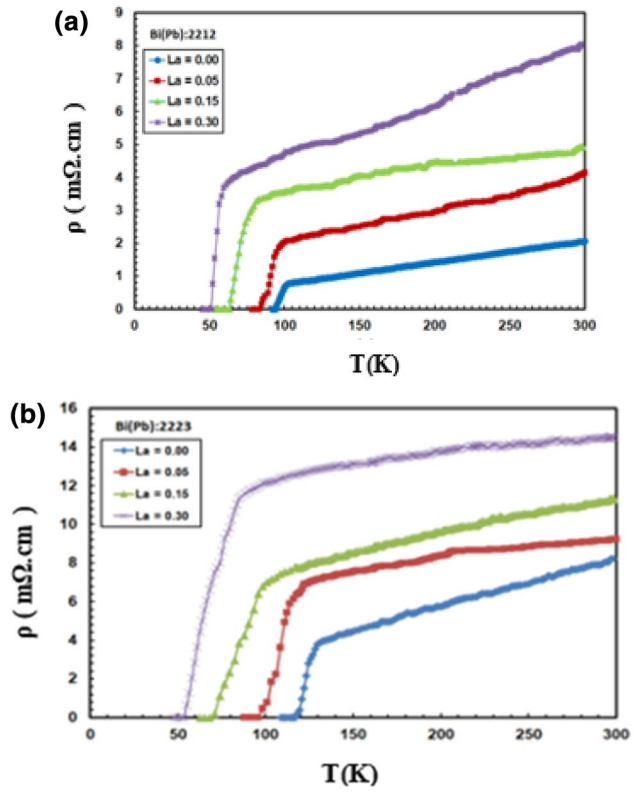

Fig. 10 Resistivity versus temperature for the samples (a) Bi (Pb) 2212 and (b) Bi (Pb) 2223.

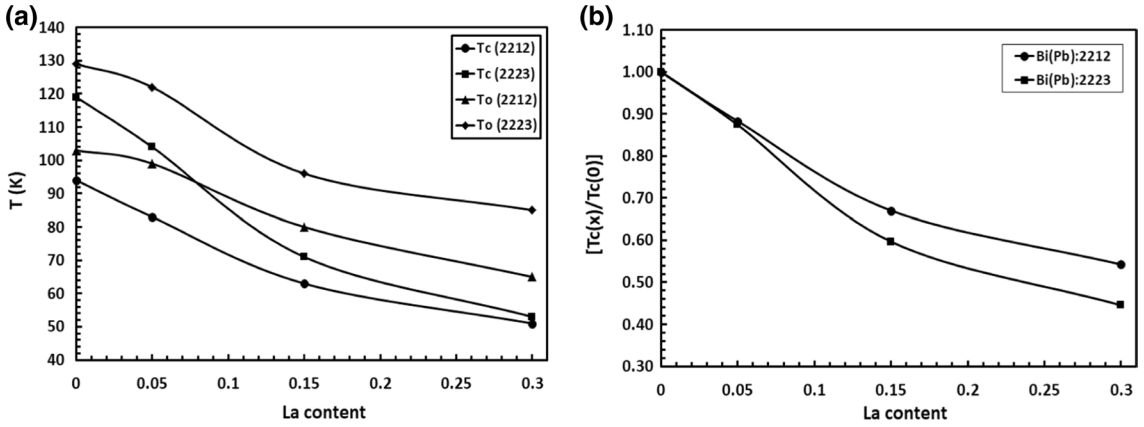

Fig. 11 (a) Critical and onset temperatures versus La content for the samples. (b) Reduced critical temperatures $[T_c(x)/T_c(0)]$ versus La content for the samples.

zero at T_{cM} for both series, the area of diamagnetic is higher than zero, indicating the presence of a superconducting state with an expected critical current, as previously reported.[59,60]

As shown in Fig. 14a and b, the onset of diamagnetism T_{cM} decreases with increasing La for both series, followed by a sharp increase to 80 K for La = 0.30 samples. T_{cM} average values for 2223 are higher than for 2212, as well as for T_{cR} ($R = 0$). Interestingly, as La increased to 0.15, the temperature difference $|T_{cM} - T_{cR}|$ also increased, and it was greater for the 2223 series than for the 2212 series. However, when La was increased to 0.30, the $|T_{cR} - T_{cM}|$ sharply increased up to 30 K for both series. This was because it was possible to determine the T_{cM} of the first islands due to pure clusters that were present essentially and appeared in the superconducting sample using high-accuracy magnetic measurements.[59,61,62] This is, of course, impossible in the case of resistivity measurements, because they are measured across the sample's cross-sectional area.

Microhardness Analysis

It is evident from the curves of microhardness H_v versus F shown in Fig. 15a and b that they were decreased by increasing F for the two series, and at fixed F, the H_v is higher for the 2212 series than the 2223 series. The higher values of H_v for 2212 are due to the decreased porosity of the 2212 series and therefore alter the point of plastic deformation.[37,63,64]

The diagonal length d_p is related F according to[15,65]

$$\frac{F}{d_p} = H_t d_p + \gamma \tag{7}$$

H_t is true hardness, and γ is surface energy. The plots of F/d_p against d_p are shown in Fig. 16a and b. Figure 17a and b shows that H_t is greater for the 2212 and 2223 series, as is H_v. But, the values of γ are higher for the 2223 series than the 2212 series, indicating that a more compacted surface

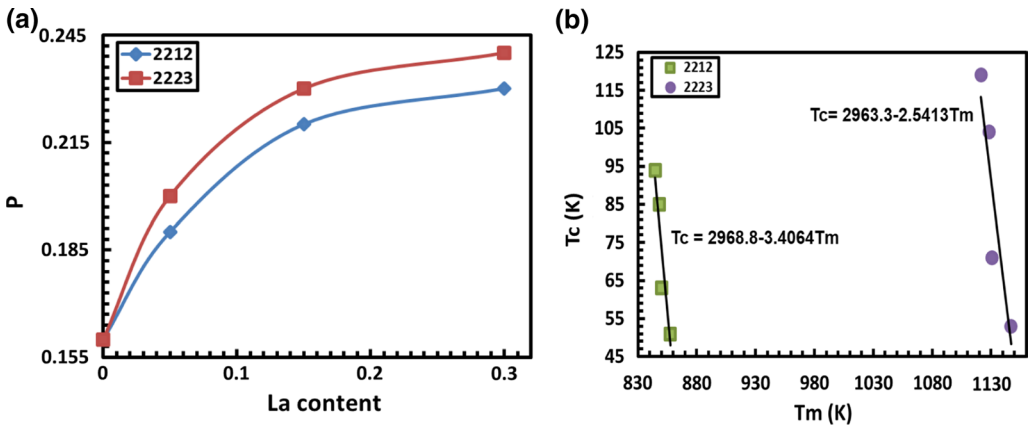

Fig. 12 (a) Hole carrier/Cu ions (P) versus La content for the samples. (b) T_c versus T_m for the samples.

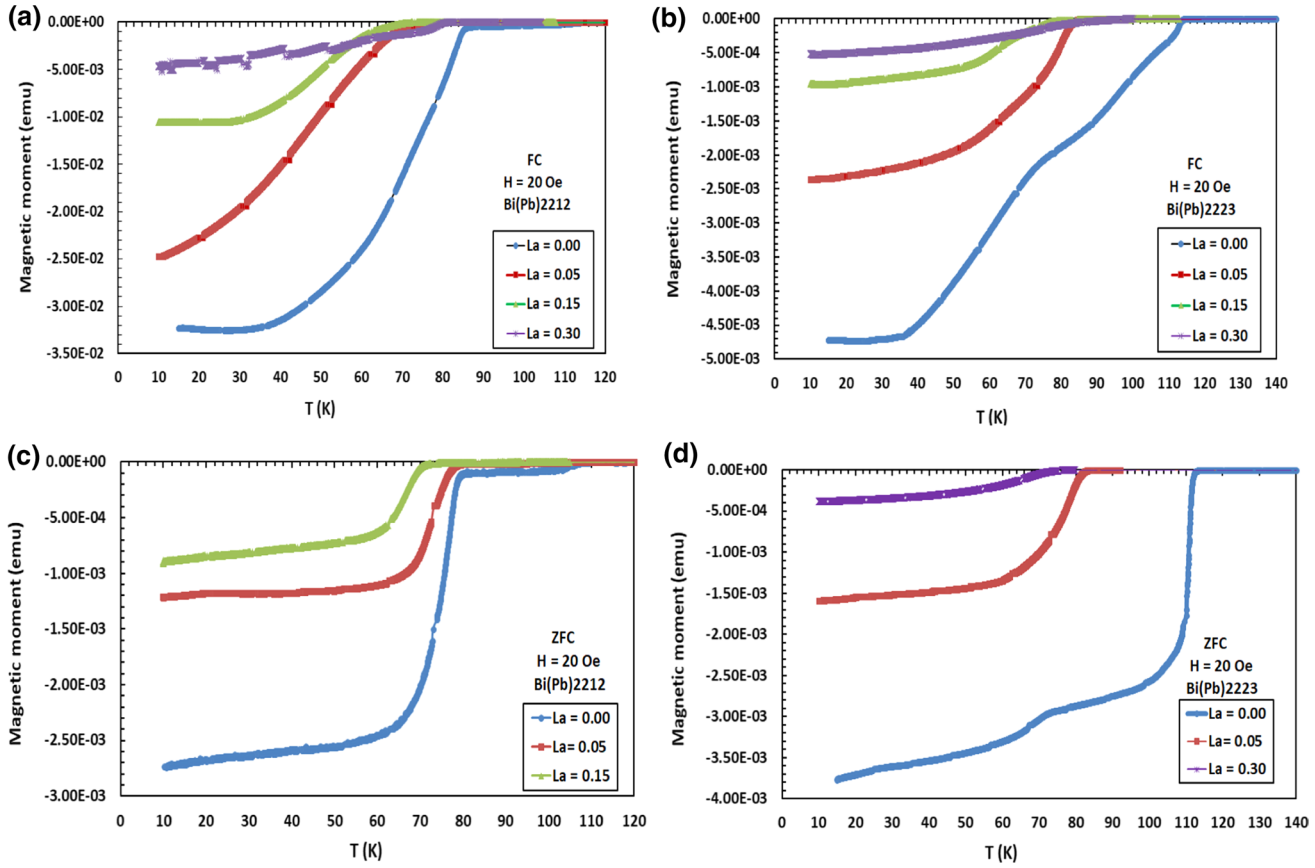

Fig. 13 Magnetic moment versus temperature for the samples (a) FC of Bi (Pb) 2212, (b) FC of Bi (Pb) 2223, (c) ZFC of Bi (Pb) 2212, and (d) ZFC of Bi (Pb) 2223.

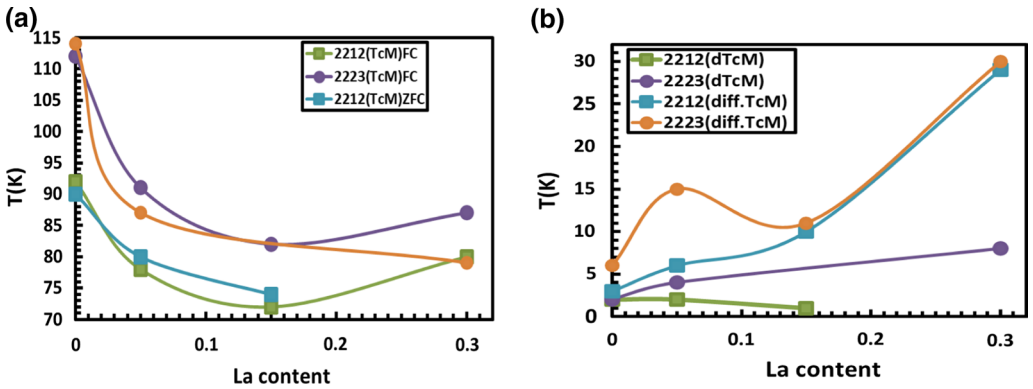

Fig. 14 (a) Onset of diamagnetism (T_{CM}) versus La content for the samples. (b) Width of transition (ΔT_{cM}) and temperature difference $|T_{cR} - T_{CM}|$ versus La content for the samples.

has higher hardness, and thus lower surface energy was obtained.

Firstly, the indentation size effect assumes that the indentation contains an elastic portion of the deformation besides plastic deformation.[66,67] This is explained by adding an elastic component d_e to the measured elastic component d_p as follows[68,69]:

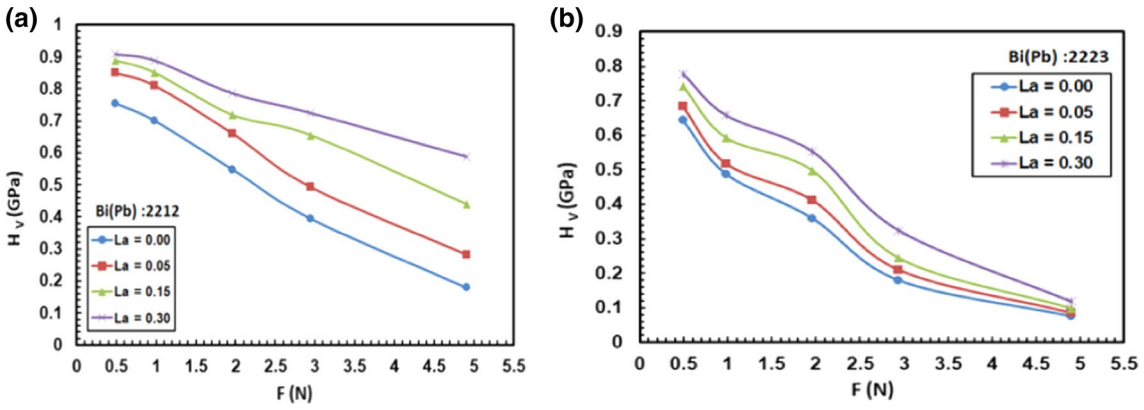

Fig. 15 Vickers hardness (H_v) against applied load (F) for the samples (a) Bi (Pb):2212 and (b) Bi (Pb):2223.

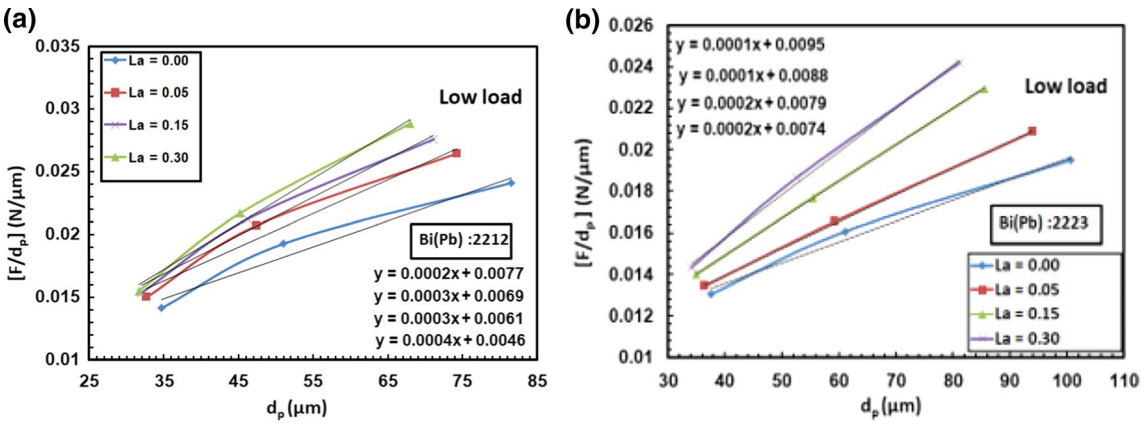

Fig. 16 The plot of F/d_p against indentation d_p for the samples (a) Bi (Pb):2212 and (b) Bi (Pb):2223.

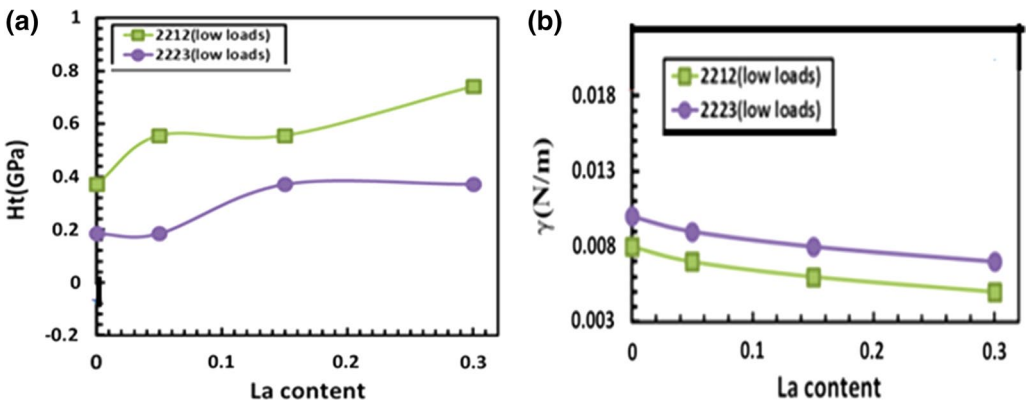

Fig. 17 (a) The plot of true hardness (H_t) against La content for the samples. (b) Surface energy (γ) against La content for the samples.

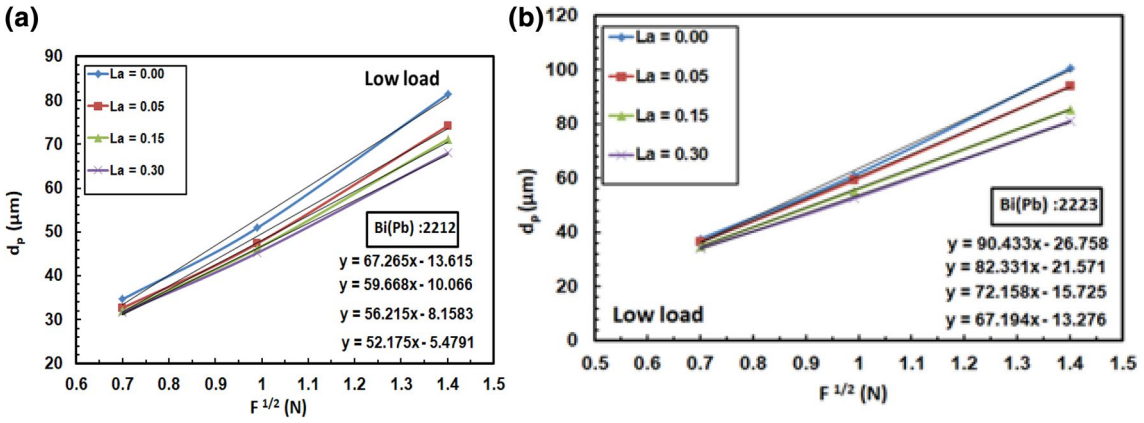

Fig. 18 Measured indentation (d_p) against applied load (F) for the samples (a) Bi (Pb) 2212 and (b) Bi (Pb) 2223.

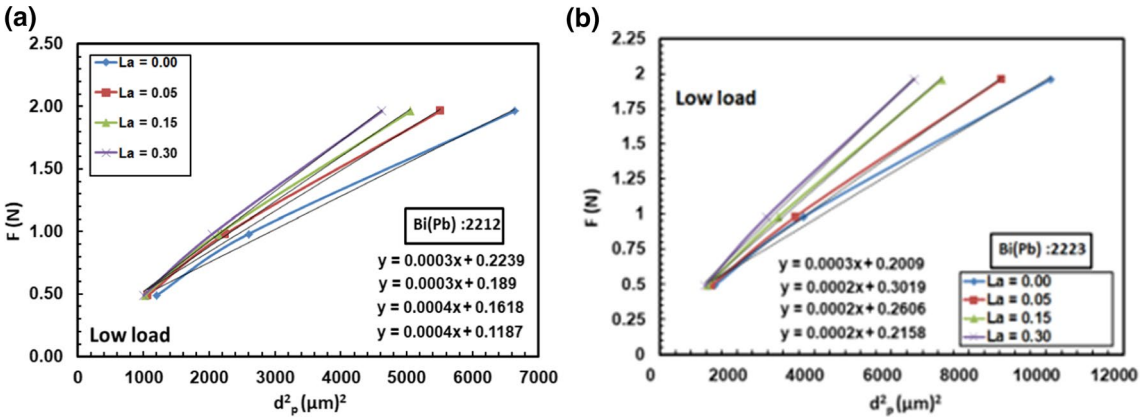

Fig. 19 Applied load (F) against indentation (d_p) for samples (a) Bi (Pb):2212 and (b) Bi (Pb):2223.

$$H_t = 1854.4\left[\frac{F}{(d_p + d_e)^2}\right]$$
$$d_p = [(1854.4)^{\frac{1}{2}} H_t^{\frac{-1}{2}}]F^{\frac{1}{2}} - d_e \quad (8)$$

The plot of d_p versus $F^{1/2}$ is shown Fig. 18a and b for the two series where the slope represents $[(1854.4)^{1/2}(H_t)^{-1/2}]$, and the vertical intercept represents d_e.

Secondly, the effect of energy dissipative processes and therefore H_t was obtained by subtracting dissipative part F_0 from applied load F as follows[70]:

$$H_t = 1854.4\left(\frac{F - F_o}{d_p^2}\right)$$
$$F = \left(\frac{H_t}{1854.4}\right)d_p^2 + F_o \quad (9)$$

The slope of the linear plot of F against d_p^2 is shown in Fig. 19a and b for the two series, in which H_t/1854.4 is the slope, and the intercept is the resistance pressure F_o. Also, Fig. 20a and b represents the behaviors of both d_e and F_o against La for both series. It is seen that they are slightly higher for the 2223 series than the 2212 series, which emphasizes the hardness suppression indicated above.

Fluctuation Analysis

The linear fit of normal resistivity ρ_n versus T, shown in Fig. 21a and b, follows the formula. The mean field temperature (T_c^{mf}) was estimated from the peak of dρ/dT against the T plot, which is shown in Fig. 22a and b. By using the values of excess conductivity $\Delta\sigma$ and reduced temperatures, ϵ, we plotted ln$\Delta\sigma$ against lnε as shown in Fig. 23a and b. However, the linear fit of each curve in the normal field region (NFR), mean field region (MFR), and critical field region (CFR) is mentioned. In Fig. 24, the crossover temperatures, T_{o1} and T_{o2}, and T_c^{mf} against La are shown in Fig. 24a and b. It is noted that their values are higher for the 2223 series than the 2212 series, as well as T_c. The interlayer coupling J and the c-axis coherence length $\xi_c(0)$ were calculated, in which $d = c/2$ for BSCCO systems as follows[71,72]:

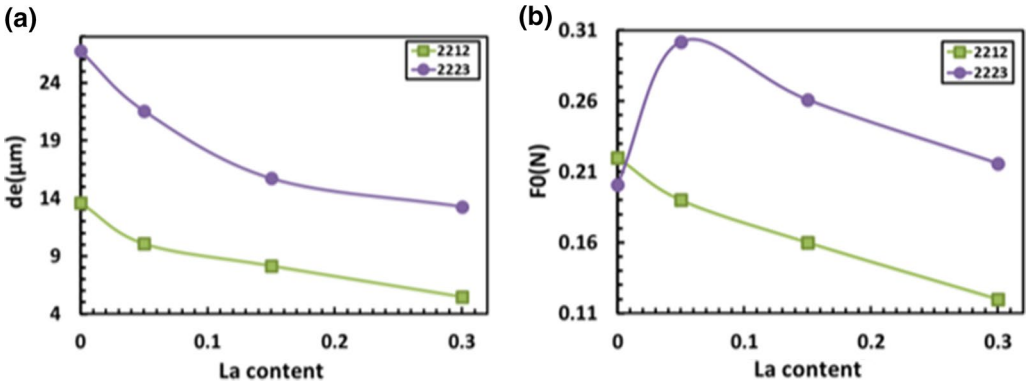

Fig. 20 (a) Elastic component (d_e) versus La content for the samples. (b) Surface energy (F_o) versus La content for the samples.

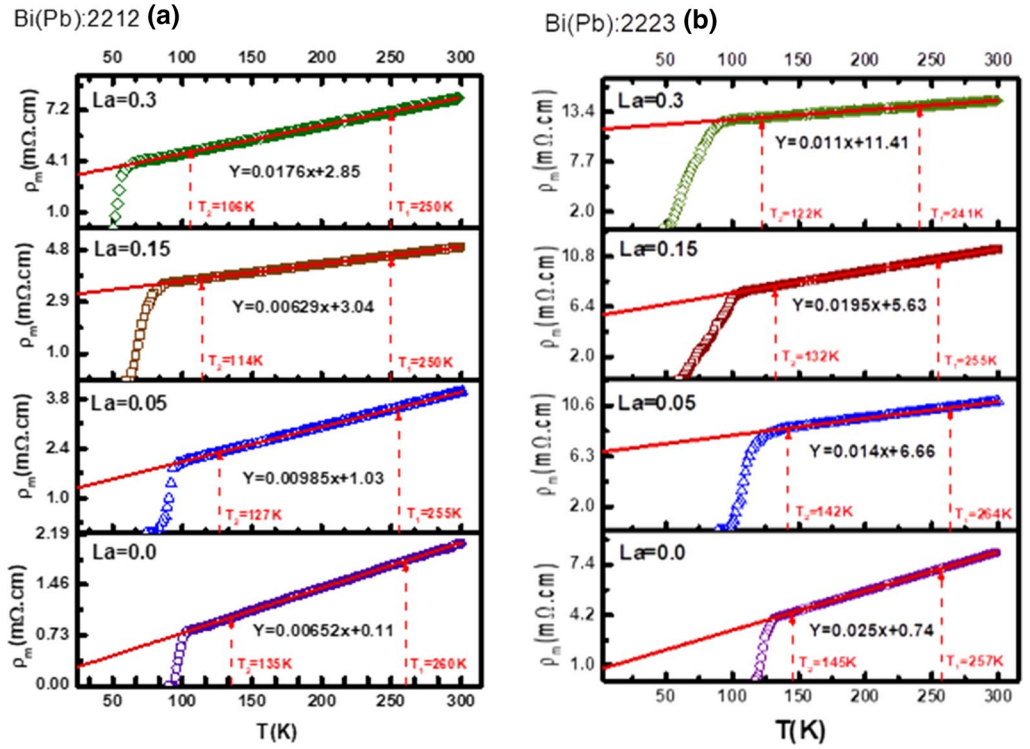

Fig. 21 The linear fit of resistivity (ρ_m) versus temperature for the samples (a) Bi (Pb):2212 and (b) Bi (Pb):2223

$$J = \ln\left(\frac{T_0}{2T_c^{mf}}\right); \quad \xi_c(0) = \left(\frac{dJ^{\frac{1}{2}}}{2}\right) \tag{10}$$

Figure 25a and b shows the behaviors of J and $\xi_c(0)$ against La content. It is clear that the values of J are higher for the 2212 series than the 2223 series, whereas the opposite is true for $\xi_c(0)$.

The dimension exponent λ was well determined using the relation $\Delta\sigma = A\epsilon^{-\lambda}$

$$\ln \Delta\sigma = \ln A - \lambda \ln \varepsilon \tag{11}$$

However, the values of λ in the CFR for the 2212 series are 0.90 (2D), 0.78 (2D), 0.70 (2D), and 0.35 (3D), whereas they are 0.53 (2D), 0.99 (2D), 0.65 (3D), and 0.38 (2D) for the 2223 series. This means that the OPD is 2D for both series, but it becomes 3D for La = 0.30 samples rather than 2D as reported for BSCOO systems.[71,72] This behavior is related to another generated reduced length

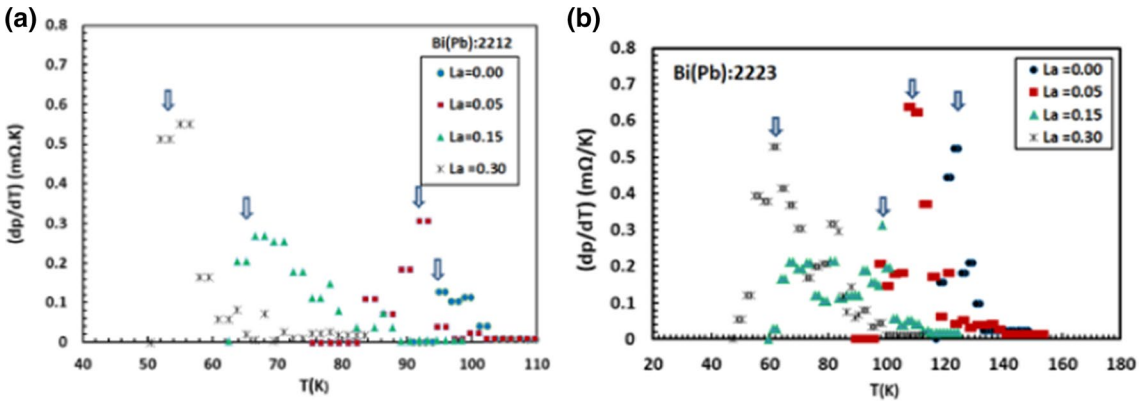

Fig. 22 (dρ/dT) versus temperature for the samples (a) Bi (Pb):2212 and (b) Bi (Pb):2223.

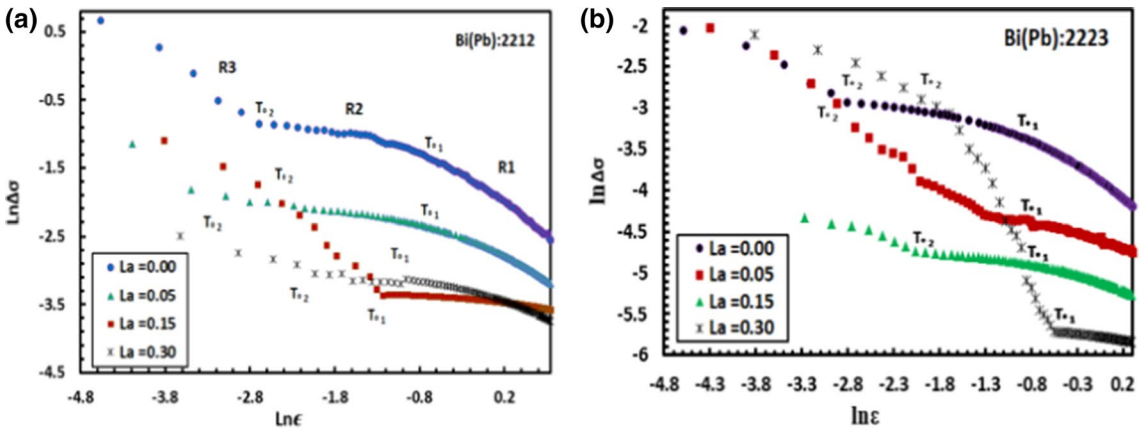

Fig. 23 Logarithmic plot of excess conductivity (ln$\Delta\sigma$) against reduced temperature (lnϵ) for the samples (a) Bi (Pb):2212 and (b) Bi (Pb):2223

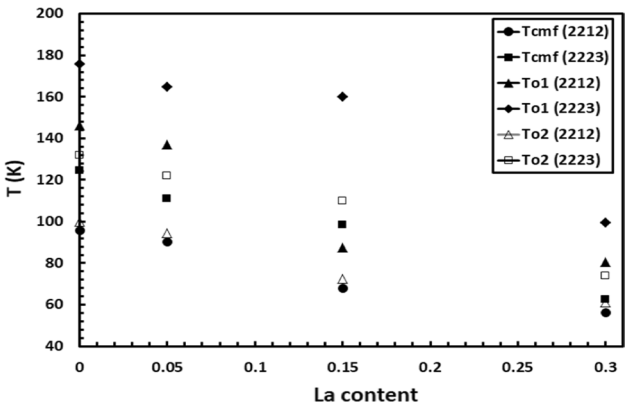

Fig. 24 Mean field and crossover temperatures (T_c^{mf} and T_o) versus La for the samples.

or dimension perpendicular to the direction of current flow.[65,73] In addition, anisotropy is given by

$$\gamma = \left[\frac{0.71K_B}{\sqrt{N_G}H_c^2(0)\xi_c^3(0)}\right]^{\frac{1}{2}} = \frac{\xi_{ab}(0)}{\xi_c(0)} \tag{12}$$

N_G is the Ginzberg reduced number given by $N_G = \frac{T_{02}-T_{cR}}{T_{cR}}$, and $H_c(0)$ is the thermodynamic critical field at 0 K given by; $H_c(0) = \frac{\varphi_0}{2\sqrt{2}\pi\lambda(0)\xi_c(0)}$, and $\lambda(0)$ is the London penetration depth at 0 K which is about 250 nm and 300 nm for 2212 and 2223 superconductors, respectively.[48]

The upper critical fields at 0 K along the c-axis $H_{c2}(c$ - axis) and along the a–b plane $H_{c2}(ab$ - plane), and also the critical current density at 0 K and $J_c(0)$ were calculated by using the following relations[74–76]:

$$H_{c2}(c\text{ - axis}) = \frac{\varphi_0}{2\pi\xi_{ab}^2(0)}; \quad H_{c2}(ab\text{ - plane}) = \frac{\varphi_0}{2\pi\xi_c(0)\xi_{ab}(0)}$$

$$H_{c2}(0) = \sqrt{[H_{c2}(ab\text{ - plane})]^2 + [H_{c2}(c\text{ - axis})]^2}$$

$$J_c(0) = \frac{2\varphi_0}{\sqrt{6}\pi\lambda^2(0)\xi_p(0)} \tag{13}$$

As indicated in Fig. 26a, the values of anisotropy are higher for the 2212 series than the 2223, while the values of NG shown in Fig. 26b are higher for the 2223 series than the 2212. On the other hand, Fig. 27a and b shows the critical field and critical current for both series, in which they are higher for the 2212 series than the 2223 series. In light of these observations, one can say that the increase in excess oxygen and hole carrier/Cu ions introduced by La into the CuO_2 planes of the BSCOO system may also affect the path of current flow in the system and improve the critical fields and currents. This leads to electronic

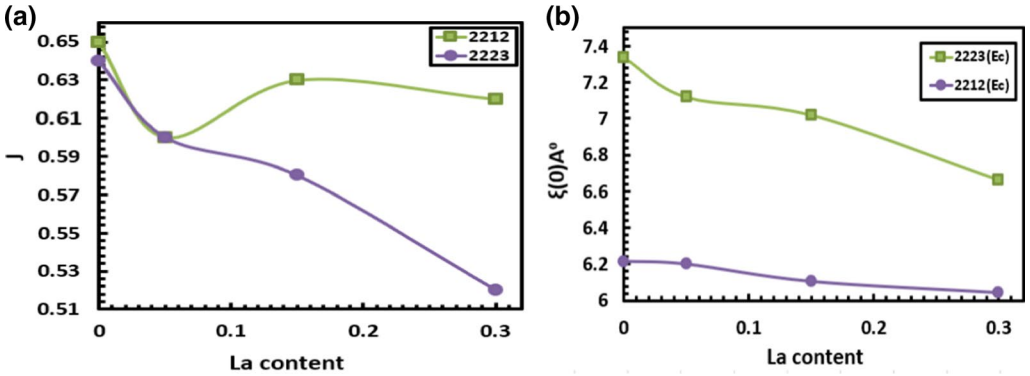

Fig. 25 (a) Interlayer coupling (J) versus La content for the samples. (b) c-axis coherence length ($\xi_c(0)$) versus La content for the samples.

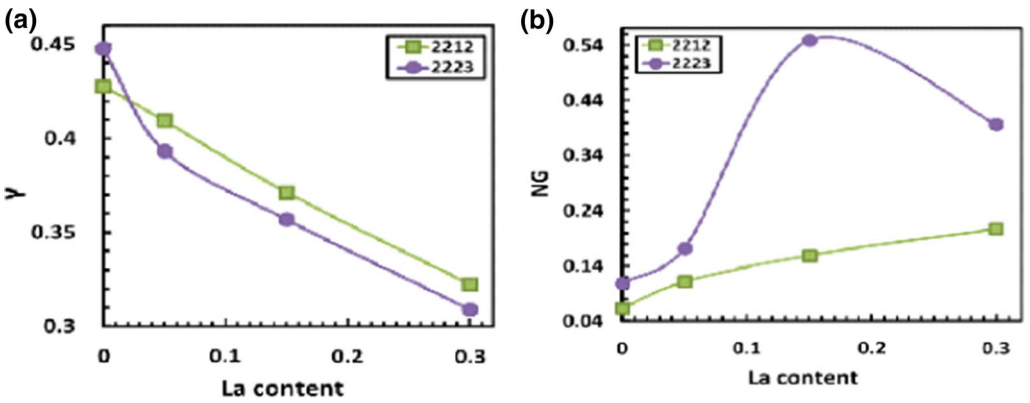

Fig. 26 (a) Anisotropy (γ) versus La content for the samples. (b) Ginzberg reduced number (N_G) versus La content for the samples.

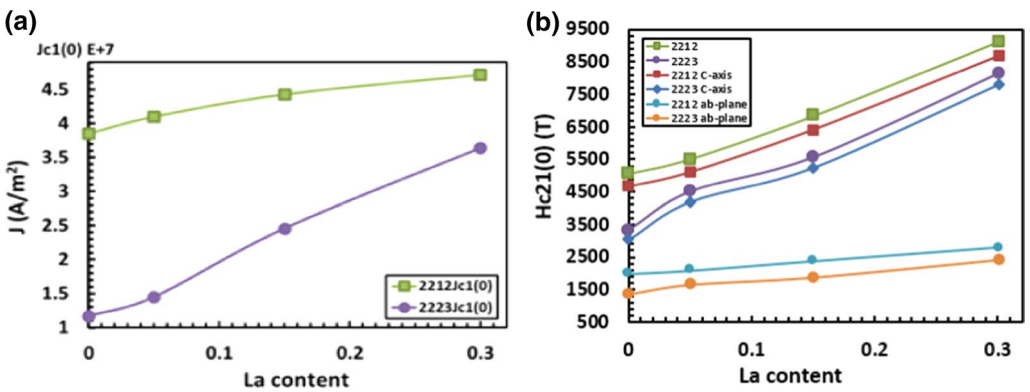

Fig. 27 (a) Critical current (J) versus La content for the samples. (b) Upper critical fields (H_{c2}) versus La content for the samples.

or chemical inhomogeneity in the charge reservoir layer (BiO/SrO), which supplies the charge carriers to the CuO_2 planes through which the actual super-current is believed to flow.[31,76,77]

However, and regardless of the effects of La discussed in detail in Refs. 29–32, it is found that x_c for quenching superconductivity, Vickers hardness, critical magnetic fields, and critical current density are higher for the 2212 series than the 2223 series. In contrast, the melting temperature T_m, critical temperature T_c, onset of diamagnetic T_{cM}, surface energy, elastic component, and resistance pressure are higher for the 2223 series than the 2212 series. These findings are due to the differences in superconducting volume fraction, crystallite diameter, porosity, excess oxygen, hole carrier/Cu ion ratio, doping distance, spacing between two neighboring Cu atoms, anisotropy, and interlayer coupling between the two series. For example, superconducting volume fraction, excess of oxygen, anisotropy, and interlayer coupling are higher for the 2212 series, and they are responsible for the former performance of the 2212 series, while the orthorhombic distortion, c-parameter, crystallite diameter, doping distance, distance between two neighboring Cu atoms, hole carrier/Cu ion ratio, and c-axis coherence length, which are higher for the 2223 series, are responsible for the latter performance of the 2223 series. To our knowledge, the present systematic investigation has not been reported elsewhere, which highlights the present work.

Conclusion

A comparative study between the effects of La-substituted Ca in (Bi, Pb):2212 and (Bi, Pb):2223 superconductors has been well investigated. We have shown that the critical concentration for quenching superconductivity, Vickers hardness, critical fields, and critical current J_c are higher for the 2212 series than the 2223 series. In contrast, the critical temperature T_c, melting temperature T_m, onset of diamagnetism T_{cM}, and resistance pressure are found to be higher for the 2223 series than the 2212 series. An inverse linear relationship between T_m and T_c could be obtained for both series. The 1048.03°C and 784.48°C T_m values are required for RT superconductors of 2223 and 2212. Surprisingly, for both series, the temperature difference between zero resistivity and diamagnetic onset, $|T_{cM} - T_{cR}|$ for La = 0.30 samples is 30 K. The order parameter exponents in the critical field region are 2D for both series, but they become 3D as La increases to 0.30 due to the expected reduced effective length in highly substituted samples. The preference of the 2212 over the 2223 for the former parameters is mainly attributed to the superconducting volume fraction, excess of oxygen, anisotropy, and interlayer coupling, which are higher for the 2212 series than the 2223 series. Meanwhile, orthorhombic distortion, c-parameter, crystallite diameter, doping distance, distance between two Cu atoms, hole carrier/Cu ion ratio, and c-axis coherence length, which are higher for the 2223 than the 2212, are responsible for the latter preference of the 2223 series. These findings reveal that the 2212 series is more suitable for applications that need higher hardness and critical fields and currents. In contrast, the 2223 series is more suitable for research for higher T_c and altering plastic deformation. To our knowledge, the present systematic investigation has not been reported elsewhere, which highlights the present work.

Acknowledgments The authors would like to thank Dr. Mahmoud Abdel-Hafiez, Harvard University, USA, and Dr. Ali Abu-Ali, Alexandria University, Egypt, for their cooperation during RT and SQUID measurements.

Funding Open access funding provided by The Science, Technology & Innovation Funding Authority (STDF) in cooperation with The Egyptian Knowledge Bank (EKB).

Conflict of interest On behalf of all authors, the corresponding author states that there is no conflict of interest.

References

1. H. Eisaki, N. Kaneko, D.L. Feng, A. Damascelli, P.K. Mang, K.M. Shen, Z.X. Shen, and M. Greven, Effect of chemical inhomogeneity in bismuth-based copper oxide superconductors. *Phys. Rev. B* 69, 064512 (2004).
2. H. Maeda, Y. Tanaka, M. Fukutomi, and T. Asano, A new high-T_cc oxide superconductor without a rare earth element. *Jpn. J. Appl. Phys.* 27, L209 (1988).
3. X.H. Chen, C. Lin, B. Lu, Y.T. Qian, L.Z. Cao, Z.J. Chen, and Z.Y. Chen, Thermodynamic stability and superconductivity of the Bi-Sr-Ca(Y)-Cu-Li-O system, *J. Mater. Res.* 8, 1510 (1993).
4. A. Amirabadizadeh, S. Memarzadeh, N. Tajabor, and H. Arabi, Effect of different calcination process and Gd_2O_3 as impurities on the different phases of bi-based superconductor. *World J. Condens. Matter Phys.* 2, 148 (2012).
5. I.H. Gul, M.A. Rehman, M. Ali, and A. Maqsood, Effect of vanadium and barium on the Bi-based (2223) superconductors. *Physica C* 432, 71 (2005).
6. H.P. Roesera, F. Hetfleischa, F.M. Huberb, M.F. von Schoenermarka, M. Steppera, A. Moritza, and A.S. Nikoghosyan, Correlation between oxygen excess density and critical transition

temperature in superconducting Bi-2201, Bi-2212 and Bi-2223, *Acta. Astronaut.* 63, 1372 (2008).
7. S.A. Halim, S.B. Mohamed, H. Azhan, S.A. Khawaldeh, and H.A.A. Sidek, Effect of barium doping in Bi–Pb–Sr–Ca–Cu–O ceramics superconductors. *Physica C* 312, 78 (1999).
8. C.A.M. dos Santos, S. Moehlecke, Y. Kopelevich, and A.J.S. Machado, Inhomogeneous superconductivity in $Bi_2Sr_2Ca_{1-x}Pr_xCu_2O_{8+\delta}$. *Physica C* 390, 21 (2003).
9. X.G. Lu, X. Zhao, X.J. Fan, X.F. Sun, W.B. Wu, and H. Zhang, Magnetization of hard superconductors. *Appl. Phys. Lett.* 76, 3088 (2000).
10. A.Y. Ilyushchkin, T. Yamashita, L. Boskovic, and I.D.R. Mackinnon, High-temperature superconductors: occurrence, synthesis and applications. *Supercond. Sci. Technol.* 17, 1201 (2004).
11. K.A. Jassim, and T.J. Alwan, The effect of simultaneous substitution of strontium at the barium site of Tl0.6Pb0.4Ba2−xSrxCa2Cu3O9−δ Superconductors. *J. Supercond. Nov. Magn.* 22, 861 (2009).
12. K.Q. Ruan, S.Y. Li, X.H. Chen, G.G. Qian, Q. Cao, C.Y. Wang, and L.Z. Cao, The systematic study of the normal-state transport properties of Bi-2212 crystals.*J. Phys. Condens. Matter* 11, 3743 (1999).
13. K. Nanda Kishore, S. Satyavathi, M. Muralidhar, O. Pena, and V. Hari Babu, Thermoelectric power studies on the Sm substituted BPSCCO (2223) superconductors. *Physica C* 252, 49 (1995).
14. A. Sedky, The impact of Y substitution on the 110 K high T_c phase in a Bi (Pb):2223 superconductors. *J. Phys. Chem. Solids* 70, 483 (2009).
15. D. Marconi, G. Stiufiuc, and A.V. Pop, Effect of partial substitution of Ca by 4f elements on dissipative processes in Bi:2223 superconductors. *J. Phys. Conf. Ser.* 153, 012022 (2009).
16. N. Hudakova, The infrared properties of Bi2Y0.1Sr1.9CaCu2O8+δ superconductor. *Physica C* 406, 58 (2004).
17. R.P. Aloysius, P. Guruswamy, and U. Syamaprasad, Highly enhanced critical current density in Pr-added (Bi, Pb)-2212 superconductor, *Supercond. Sci. Technol.* 18, 5, L23 (2005).
18. Q. Cao, K.Q. Ruan, S.Y. Li, X.H. Chen, G.G. Qian, and L.Z. Cao, The comparable effects on transport properties in Bi2Sr2Ca1-xPrxCu2Oy and Bi2Sr2Ca1-xYxCu2Oy single crystals. *Physica C* 334, 237 (2000).
19. S.M. Khalil, Effect of Y^{3+} substitution for Ca on the transport and mechanical properties of $Bi_2Sr_2Ca_{1-x}Y_xCu_2O_{8+\delta}$ system. *J. Phys. Chem. Solids* 64, 855 (2003).
20. X. Sun, X. Zhao, W. Wu, X. Fan, X.G. Li, and H.C. Ku, Pr-doping effect on the structure and superconductivity of Bi2Sr2Ca1−xPrxCu2Oy single crystals. *Physica C* 307, 7 (1998).
21. M. Yilmazlar, H.A. Cetinkara, M. Nursoy, O. Ozturk, and C. Terzioglu, Thermal expansion and Vickers hardness measurements on Bi1.6Pb0.4Sr2Ca2-xSmxCu3Oy superconductors. *Physica C* 442, 101 (2006).
22. A. Sedky, On the influence of rare-earth substitution for Ca in superconducting system. *Physica C* 468, 1041 (2008).
23. J. Hwang, T. Timusk, and G.D. Gu, High-transition-temperature superconductivity in the absence of the magnetic-resonance mode. *Nature* 427, 714 (2004).
24. M. Norman, Copper oxides superconductors at unusually high temperatures. New evidence from optical studies highlights the nature of the many-body interactions involved. *Nature* 427, 692 (2004).
25. P. Sumana Prabhu, M.S. RamachandraRao, U.V. Varadaraju, and G.V. SubbaRao, Tc suppression and conduction mechanisms in Bi2.1Sr1.93Ca0.97−xRxCu2O8+y (*R*=Pr, Gd, and Er) systems. *Phys. Rev. B* 50, 6929 (1994).
26. V.P.S. Awana, S.K. Agarwal, R. Ray, S. Gupta, and A.V. Narlikar, Superconductivity and resistivity studies in $Bi_2Sr_2Ca_{1-x}M_xCu_2O_{8+y}$ (M=Eu, Dy, Tm and $0 \leq x \leq 0.6$). *Physica C* 43, 191 (1992).
27. J.M. Tarason, P. Barboux, G.W. Hull, R. Ramesh, L.H. Greene, M. Giroud, M.S. Hegde, and W.R. Mckinnon, Bismuth cuprate high-Tc superconductors using cationic substitution. *Phys. Rev. B* 39, 4316 (1989).
28. K. Koyama, S. Kanno, and S. Noguchi, Electrical, magnetic and superconducting properties of the quenched Bi2Sr2Ca1-xNdx-Cu2O8+ δ system. *Jpn. J. Appl. Phys.* 29, L53 (1990).
29. A. Sedky, A. Salah, A.A. Bahgat, and A. Abou-Aly, Cooperative effects due to Ca substitution by La on the normal and superconducting states of (Bi, Pb):2223 system. *J. Mater. Sci. Mater. Electron.* 31, 12502 (2020).
30. A. Sedky, A. Salah, and A. Abou-Aly, Normal and superconducting properties of Bi1.7Pb0.30Sr2Ca1−xLaxCu2Oy superconductor with $0.00 \leq x \leq 0.30$. *J. Supercond. Nov. Magn.* 33, 3349 (2020).
31. A. Sedky, and A. Salah, Excess conductivity, diamagnetic transition and FTIR spectra of Ca substituted by La in (Bi,Pb):2212 superconducting system. *J. Low Temp. Phys.* 201, 294 (2020).
32. A. Sedky, and A. Salah, Fluctuation, diamagnetic transition and FTIR spectra of Ca substituting La in (Bi,Pb):2223 superconducting system. *J. Supercond. Nov. Magn.* 33, 3705 (2020).
33. M.S. Lee, and K.Y. Song, Effect of Nd substitution for the Ca site in the 110 K phase of (Bi, Pb)–Sr–Ca–Cu–O superconductors. *Supercond. Sci. Technol.* 15, 851 (2002).
34. S.M. Khalil, and A. Sedky, Annealing temperature effect on the properties of Bi: 2212 superconducting system. *Physica B* 357, 299 (2005).
35. A. Simon, P.S. Mukherjee, M.S. Sarma, and A.D. Damodaran, Variation of structural and superconducting properties with initial stoichiometry variation in (Bi, Pb)-Sr-Ca-Cu-O bulk superconductor. *J. Mater. Sci.* 29, 5059 (1994).
36. G. Blatter, M.V. Feigel'man, V.B. Geshkenbein, A.I. Larkin, and V.M. Vinokur, Vortices in high-temperature superconductors. *Rev. Mod. Phys.* 66, 1125 (1994).
37. M. Yilmazlar, H.A. Cetinkara, M. Nursoy, O. Ozturk, and C. Terzioglu, Thermal expansion and vickers hardness measurements on Bi1.6Pb0.4Sr2Ca2-xSmxCu3Oy superconductors. *Phys. C Supercond.* 442, 101 (2006).
38. S. Singh, Suppression of superconductivity in Sm and Co substituted Bi2Sr2Ca1Cu2O8+δ system. *Phys. C Supercond.* 294, 249 (1998).
39. A. Sedky, The impact of Y substitution on the 110K high Tc phase in a Bi (Pb):2223 superconductor. *J. Phys. Chem. Solids* 70, 483 (2009).
40. M.A. Aksan, and M.E. Yakinci, Effect of Mo substitution on the structural and transport properties of Bi2Sr2Ca2Cu3-xMoxO10+y system. *J. Alloys Compd.* 433, 22 (2007).
41. C.H. Hwang, and G. Kim, Crystallization of a Bi-Pb-Sr-Ca-Cu-O system prepared by a melt process. *Supercond. Sci. Technol.* 5, 586 (1992).
42. S. Qayyum, S.K. Durrani, J. Akhtar, A.H. Qureshi, M. Arif, M. Ahmed, and S. Rahman, Formation of low TC superconducting phase in BSCCO system. *Nucleus* 45, 33 (2008).
43. S.K. Durrani, A.H. Qureshi, S. Qayyum, and M. Arif, Development of superconducting phases in BSCCO and Ba-BSCCO by sol spray process. *J. Therm. Anal. Calorim.* 95, 87 (2009).
44. S.H. Jamil, A. Hashim, S.Y.S. Yahya, A. Kasim, N.H. Hasan, and N.A. Wahab, Analysis of thermogravimetric (TG) and infra-red (FTIR) on dy substitution in Bi(Pb)-2223 superconductor. *Malays. J. Anal. Sci.* 19, 1284 (2015).
45. R.P. Aloysius, P. Guruswamy, and U. Syamaprasad, Highly enhanced critical current density in Pr added (Bi, Pb)-2212 superconductor. *Supercond. Sci. Technol.* 18, L23 (2005).

46. S. Bernik, M. Hrovat, and D. Kolar, The thermal stability of Bi superconductors in the Bi(Pb)-Sr-Ca-Cu-O system, Supercond. *Supercond. Sci. Technol.* 7, 920 (1994).
47. A. Wada, N. Suzuki, A. Maeda, S. Uchida, K. Uchinokawa, and S. Tanaka, Preparation of high-T_c (110 K) superconducting phase by the annealing of low-T_c (80 K) superconductor $Bi_2(Sr_{0.5}Ca_{0.5})_{3-x}Cu_2O_y$. *Jpn. J. Appl. Phys.* 27, L545 (1988).
48. A. Broido, sensitive graphical method of treating thermogravimetric analysis data. *J. Polym. Sci. Part A-2 Polym. Phys.* 7, 1761 (1969).
49. F. Jean, G. Collin, M. Andrieux, N. Blanchard, and J.F. Marucco, Oxygen nonstoichiometry, point defects and critical temperature in superconducting oxide Bi 2Sr 2CaCu 2O 8+ Δ. *Physics C* 339, 269 (2000).
50. M.R. Norman, H. Ding, M. Randeria, J.C. Campuzano, T. Yokoya, T. Takeuchi, T. Takahashi, T. Mochiku, K. Kadowaki, P. Guptasarma, and D.G. Hinks, Destruction of the Fermi surface in underdoped high-T_c superconductors. *Nature* 392, 157 (1998).
51. J.W. Alldredge, J. Lee, K. McElroy, M. Wang, K. Fujita, Y. Kohsaka, C. Taylor, H. Eisaki, S. Uchida, P.J. Hirschfeld, and J.C. Davis, Evolution of the electronic excitation spectrum with strongly diminishing hole density in superconducting $Bi_2Sr_2CaCu_2O_{8+}$. *Nat. Phys.* 4, 319 (2008).
52. H.P. Roesera, F.M. Huberb, M.F. von Schoenermarka, and A.S. Nikoghosyanc, Nikoghosyanc, High temperature superconducting with two doping atoms inLa-doped Bi-2201 and Y-doped Bi-2212Acta Astronautica. *Acta Astronaut.* 65, 489 (2009).
53. S. Bal, M. Dogruer, G. YilDirim, A. Varilci, C. Terzioglu, and Y. Zalaoglu, Role of cerium addition on structural and superconducting properties of Bi-2212 system, *J. Supercond. Nov. Magn.* 25, 847 (2012).
54. B.T. Matthias, The empirical approach to superconductivity, Chapter 7, *Applied Solid State Physics*. ed. W. Low, and M. Schieber (New York: Plenum Press, 1970). https://doi.org/10.1007/978-1-4684-1854-5.
55. A.A. Bahgat, High Tc Updata (USA) Technical Report 6, 19 (1992).
56. M.R. Presland, J.L. Tallon, R.G. Buckley, R.S. Liu, and N.E. Flower, General trends in oxygen stoichiometry effects on T_c in Bi and Tl superconductors. *Physica C* 176, 95 (1991).
57. P. Konsin, and B. Sorkin, Dependences of the chemical potential shift and superconducting transition temperature on the hole concentration in La2-xSrxCuO4 and Bi2Sr2Ca1-xYxCu2O8+delta. *Supercond. Sci. Technol.* 13, 301 (2000).
58. A. Leenders, M. Mich, and H.C. Freyhardt, Influence of thermal cycling on the mechanical properties of VGF melt-textured YBCO. *Physica C* 279, 173 (1997).
59. S. Khalil, Effect of Y3+ substitution for Ca on the transport and mechanical properties of Bi2Sr2Ca1-xYxCu2O8+δ system. *J. Phys. Chem. Solids* 64, 855 (2003).
60. M.A. Aksan, S. Altin, M.E. Yakinci, A. Guldeste, and Y. Balci, Effect of Bi deficiency on grain alignment of Bi(Pb)-2223 thin film fabricated using Rf sputtering process and on critical current density properties. *Mater. Sci. Technol.* 27, 314 (2011).
61. S. Altin, M.A. Aksan, and M.E. Yakinci, Fabrication of single crystalline Bi-2212 whiskers from Ga added Bi2Sr2Ca2Cu3Ox composition and their thermal, structural, electrical and magnetic properties. *Mater. Chem. Phys.* 133, 706 (2012).
62. H. Jin, and J. Kötzler, Effect of La doping on growth and superconductivity of Bi-2212 crystals. *Phys. C Supercond.* 325, 153 (1999).
63. G. Xu, Q. Pu, B. Liu, J. Zhang, C. Zhang, Z. Ding, and Y. Zhang, Different Tc-suppression rates between Mn doped La214 and Bi2201 systems. *Phys. C Supercond.* 390, 75 (2003).
64. J.C. Phillips, Slow dynamics in glasses: a comparison between theory and experiment. *Phys. Rev. B* 73, 104206 (2006).
65. W. Schnelle, E. Braun, H. Broicher, H. Weiss, H. Geus, S. Ruppel, M. Galffy, W. Braunisch, A. Waldorf, F. Seidler, and D. Wohlleben, Superconducting fluctuation In Bi2Sr2Ca2Cu3Ox. *Phys. C Supercond.* 161, 123 (1989).
66. R.K. Nkum, and W.R. Datars, Weak link in ceramic in doped Bi-Pb-Sr-Ca-Cu-O. *Supercond. Sci. Technol.* 8, 822 (1995).
67. A. Biju, R.G. AbhilashKumar, R.P. Aloysius, and U. Syamaprasad, Structural and superconducting properties of Bi1.7Pb0.4Sr2-xYbxCa1.1Cu2.1Oy system. *Phys. C Supercond. Appl.* 449, 109 (2006).
68. A. Sedky, A. Gupta, V.P.S. Awana, and A.V. Narlikar, Structural and superconducting properties of R1-xCaxBa2Cu3O7-y with 0.50>x>0.00. *Phys. Rev. B* 58, 12495 (1998).
69. A. Leenders, M. Mich, and H.C. Freyhard, Influence of thermal cycling on the mechanical properties of VGF melt-textured YBCO. *Phys. C Supercond.* 279, 173 (1997).
70. A. Galluzzi, M. Polichetti, K. Buchkov, E. Nazarova, D. Mancusi, and S. Pace, Evaluation of the intragrain critical current density in a multidomain FeSe crystal by means of DC magnetic measurements. *Supercond. Sci. Technol.* 28, 115005 (2015).
71. P.K. Maheshwari, L.M. Joshi, B. Gahtori, A.K. Srivastava, A. Gupta, S.P. Patnaik, and V.P.S. Awana, Flux free growth of superconducting FeSe single crystals. *Mater. Res. Express* 3, 076002 (2016).
72. S. Vinu, P.M. Sarun, A. Biju, R. Shabna, P. Guruswamy, and U. Syamaprasad, The effect of substitution of Eu on the critical current density and flux pinning properties of (Bi, Pb)-2212 superconductor. *Supercond. Sci. Technol.* 21, 045001 (2008).
73. X. Zhao, X. Sun, X. Fan, W. Wu, X.-G. Li, S. Guo, and Z. Zhao, Correlation between Tc And ns/m* In Bi2Sr2CaCu2O8+δ single crystals. *Phys. C Supercond.* 307, 265 (1998).
74. S. Ravi, and V. Seshu Bai, Ac-susceptibility study of the 110-K superconducting phase of Bi-Sr-Ca-Cu-O. *Phys. Rev. B* 49, 13082 (1994).
75. A. Sedky, On the study of Müllers model in high-temperature superconductors. *J. Magn. Magn. Mater.* 277, 293 (2004).
76. N.A. Khan, N. Hassan, S. Nawaz, B. Shabbir, S. Khan, and A.A. Rizvi, Effect of Sn substitution on the para-conductivity of polycrystalline Cu0.5Tl0.5Ba2Ca2Cu3−ySnyO10−δ superconductors. *J. Appl. Phys.* 107, 0839 (2010).
77. G. Pei, C. Xia, S. Cao, J. Zhang, F. Wu, and J. Xu, Synthesis and magnetic properties of Ni-doped zinc oxide powders. *J. Magn. Magn. Mater.* 302, 340 (2006).